Materials Research Express

PAPER

Optical properties of HfO_x ($x < 2$) films grown by ion beam sputtering-deposition method

To cite this article: A K Gerasimova *et al* 2019 *Mater. Res. Express* **6** 016423

Materials Research Express

PAPER

Optical properties of HfO_x ($x < 2$) films grown by ion beam sputtering-deposition method

RECEIVED
30 July 2018

REVISED
27 August 2018

ACCEPTED FOR PUBLICATION
2 October 2018

PUBLISHED
26 October 2018

A K Gerasimova, V Sh Aliev, V N Kruchinin, I A Badmaeva, V A Voronkovskii and S G Bortnikov
Rzhanov Institute of Semiconductor Physics SB RAS, 13 Lavrentiev Aven., 630090, Novosibirsk, Russia
E-mail: gerasimova@isp.nsc.ru

Keywords: HfOx, ReRAM, spectroscopic ellipsometry, IBSD

Abstract

The optical properties of the HfO_x films of different chemical composition ($x \leqslant 2$) deposited by ion beam sputtering-deposition (IBSD) method were studied. Spectral dependencies of refractive index $n(\lambda)$ and extinction coefficient $k(\lambda)$ were determined with ellipsometry in $\lambda = 250$–1100 nm wavelength region. The x values (i.e. [O]/[Hf] ratio) for the films were derived from x-ray photoelectron spectroscopy (XPS) data. The spectral dependences of optical constants $n(\lambda)$ and $k(\lambda)$ were found to undergo radical changes with $x = 1.78$–1.82. The films with $x < 1.78$ demonstrated high extinction coefficient $k > 1$ with the metallic-like behavior of optical constants spectral dependences. The films with $x > 1.82$ were found to be transparent, with $k = 0$ and $n(\lambda)$ being well approximated by a Cauchy polynomial dependence for dielectrics. Using a sample with a gradient of x, it was established that the transition from the metallic to the dielectric-like behavior of the optical constants occurs not smoothly, but is discontinuous. A sharp jump in the optical constants is observed at $x \approx 1.8$. According to XPS data, the transparent films were found to consist of two components only: HfO_2 and Hf_4O_7 suboxide. Cauchy polynomial coefficients for Hf_4O_7 suboxide and HfO_2 were found by using the Bruggeman effective medium approximation.

1. Introduction

The transition metal oxide films are widely used in microelectronic applications and optical coatings technology [1–4] and, therefore, optical and electrical properties of these films are well studied. However, non-stoichiometric transition metal oxide films are not studied enough as they generally represent dispersed systems consisting of several phases with different properties. Nevertheless, such films have attracted a lot of interest as they are capable of multiple resistive switching enabling creation of new non-volatile resistive memory known as ReRAM [5–7]. One of the most promising materials for ReRAM is hafnium oxide HfO_x ($x < 2$). The x value depends on the film growth conditions and greatly affects ReRAM cell electrical properties. Therefore, it is important to determine x, and it was done in our previous work by XPS method for the films synthesized by the ion beam sputtering-deposition (IBSD) method with different x values [8]. In this work the optical method is used for determining the x values for these films.

2. Experimental technique

2.1. Films synthesis

HfO_x films of different chemical composition were grown by the IBSD method on n-type Si (100) substrates ($\rho = 4.5\ \Omega \times$ cm) at room temperature. Before deposition the substrates were precleaned in a hydrofluoric acid (HF) solution. The metallic hafnium (Hf $> 99.9\%$) target was sputtered by Ar^+ ions with energy of 1.2 keV and current density of about 1 mA cm^{-2}. The composition of HfO_x was set by the O_2 (high purity $O_2 > 99.999\%$) partial pressure varied in 0.4×10^{-3}–4.0×10^{-3} Pa range. The detailed synthesis procedure and films

characterization by XPS and field emission scanning electron microscopy (FESEM) methods were previously described [8].

A sample with a gradient of oxygen concentration along the surface of the HfOx film was also prepared. To create a gradient, the Si (100) substrate with a size of 10 × 15 mm^2 was unfolded relative to the particle flow coming from the sputtered target. As a result, a HfO_x film was formed with a gradient of oxygen concentration along the film surface. However, the film was also obtained with a thickness gradient. For an independent determination of the thickness gradient, an additional sample was also grown with the same unfolding of the substrate, but an excess flow of oxygen molecules was fed into the chamber. This led to the growth of a film of HfO_2 composition on the entire surface of the sample, but with a gradient of thickness. The thickness gradient obtained on the additional sample was then used to unambiguously approximate the ellipsometry data of the sample with a gradient of oxygen concentration in the film.

2.2. The optical properties of HfO_x films

The wavelength-dependent refractive index $n(\lambda)$ and extinction coefficient $k(\lambda)$ were determined by means of spectroscopic ellipsometry (SE) [9, 10]. Ellipsometric angles Ψ and Δ were measured as a function of λ in the 250–1100 nm spectral range by using the ELLIPSE-1891-SAG ellipsometer [11]. The instrumental spectral resolution was 2 nm, and the recording time of the spectrum did not exceed 20 s. The SE measurements were performed at three light beam incidence angles 50°, 60° and 70°. The four-zone measurement method was used with subsequent data averaging over all four zones. Ellipsometric parameters Ψ and Δ are related to the complex Fresnel reflection coefficients by the equation (1):

$$tg\,\Psi \cdot e^{i\Delta} = \frac{R_p}{R_s}, \tag{1}$$

where R_p and R_s are the coefficients for p- and s-polarized light waves. The spectral dependences of ellipsometric parameters Ψ and Δ can be fitted with appropriate models to extract the film thickness and the optical constants $n(\lambda)$ and $k(\lambda)$ based on the best matching of experimental and simulated spectra [10–14]. To calculate the wavelength dependences of refractive index $n(\lambda)$ and extinction coefficient $k(\lambda)$, the experimental data were processed by using both the single-layer model (air/homogeneous isotropic layer/homogeneous isotropic substrate) for transparent films and the semi-infinite model (air/homogeneous isotropic substrate) for opaque films. Thus, the spectral dependences of polarization angles were fitted for all m points in the spectrum by the error function minimization

$$\sigma^2 = \frac{1}{m} \cdot \sum_{i=1}^{m} [(\Delta_{\text{exp.}} - \Delta_{calc.})^2 + (\Psi_{\text{exp.}} - \Psi_{calc.})^2]. \tag{2}$$

Dispersion function $n(\lambda)$ for transparent films was approximated by Cauchy polynomial

$$n(\lambda) = a + \frac{b}{\lambda^2} + \frac{c}{\lambda^4}, \tag{3}$$

where a, b, and c—the constants specific for the material, with $k(\lambda)$ assumed to be zero. For opaque films the dispersion functions $n(\lambda)$ and $k(\lambda)$ were calculated from the relation $\varepsilon(E) = N(E)^2$, where $N(E) = n(E)$-$ik(E)$ is the complex refractive index, and the Lorentz-Drude approximation for the complex dielectric function dependence on photon energy was used [15]

$$\varepsilon(E) = \varepsilon_\infty - \frac{E_{1D}^2}{E^2 - iE_{2D}E} + \sum_{i=1}^{l} \frac{A_n E_n^2}{E_n^2 - E^2 + i\Gamma_n E_n E}, \tag{4}$$

where $E = \frac{hc}{\lambda}$—photon energy, h—Planck constant, c—the light speed in vacuum, $i = \sqrt{-1}$, and ε_∞—value of $\varepsilon(E)$ at $E \to \infty$. The second term of (4) reflects the contribution of Drude free carriers, where E_{1D} and E_{2D} are constants. The third Lorentzian term describes the contribution of interband transitions as excitations of damped harmonic oscillators, where A_n, E_n and Γ_n are the strength, energy, and broadening function of the n-th oscillator from l oscillators used in the calculation, respectively.

Optical constants (n, k) profiles of the gradient films deposited on to the 15 × 10 mm^2 Si substrates were measured by means of laser ellipsometry using a 'Microscan' high spatial resolution ellipsometer (the Rzhanov Institute of Semiconductor Physics of the SBRAS, Russia) [16]. Ellipsometric angles were measured at the wavelength of 632.8 nm, and the incidence angle of the light beam with respect to the sample was equal to 60°. The spatial resolution in the scanning mode amounted to about 10 μm.

Table 1. Experimental growth conditions for HfO_x films. P_{O2}—O_2 partial pressure, R—the growth rate measured by the quartz crystal microbalance with a fixed layer material volumetric mass density, t—deposition time. x coefficient reflects the composition of HfO_x films according to XPS data [8].

Sample	$P_{O2}(\times 10^{-3}$ Pa)	R (nm/s)	t (s)	x
#1	0.44	0.11	435	1.42
#2	0.62	0.12	407	1.52
#3	1.0	0.13	373	1.67
#4	1.8	0.12	410	1.82
#5	3.1	0.065	765	1.87
#6	3.6	0.049	1027	1.92

3. Results and discussion

The 6 samples to be investigated were grown at various O_2 partial pressures. The experimental films growth conditions are presented in table 1. The growth rate R was determined by the quartz crystal microbalance (TM-400, MAXTEC) with a constant material volumetric mass density. The density was set equal to the metallic hafnium one (13.09 g cm^{-3}) and, therefore, the measured growth rate was incorrect corresponding to the film weight rate but not its thickness.

The results of film optical properties measurements by SE are shown in figure 1. It appeared the dependences $\Psi(\lambda)$ and $\Delta(\lambda)$ of the samples are qualitatively different and the samples can be divided into two groups. The films of group 1 (samples #1–3) strongly absorb light. The minimum error function σ^2 approximating experimental curves $\Psi(\lambda)$ and $\Delta(\lambda)$ was obtained using a semi-infinite medium model with the Lorentz-Drude dispersion of optical constants. The real n and imaginary k parts of the complex refractive index dependence on photon energy E for HfO_x films of group 1 are shown in figure 2, and the parameters of Drude-Lorentz model are in table 2. The area between the two dashed lines for each experimental curve corresponds to the 5% accuracy for the chosen Drude-Lorentz model parameters. It is clear that, while samples #1 and #2 satisfactorily fit the area between the dashed lines, the sample #3 is substantially away from this area at high photon energies. Probably, in this case, the model of semi-infinite medium is not applicable. Indeed, the evaluation of the optical penetration depth $D = \frac{3\lambda}{4\pi k}$ at $\lambda = 632.8$ nm gives 50.7 nm, 54.8 nm and 105.7 nm for samples #1, 2 and 3, respectively, and the film thicknesses defined by experimental growth conditions were about 80 nm. Therefore, the semi-infinite model is suitable for the first two samples, but not for the third one. In case of sample #3, the use of the semi-infinite model gives an error in dispersion functions calculation not exceeding 15%. Strong absorption and monotonic decrease of refractive index at high photon energies are typical for many metals [17]. For comparative purposes the optical constants of pure hafnium metal was measured by SE. The hafnium surface was preliminarily polished, etched and degreased in a solution based on HF and nitric acids. One can see in figure 2 that the spectral dependence of the optical constants $n(E)$ and $k(E)$ of HfO_x films #1 and #2 correlate well with the ones for the metal hafnium.

The films of group 2 (samples #4–6) were transparent and, therefore, optical constants $n(\lambda)$ and $k(\lambda)$ were calculated within the single-layer model (figure 3). The best result for error function σ^2 was obtained when $n(\lambda)$ was approximated by Cauchy polynomial [18], with $k(\lambda) = 0$. As an example, figure 1 shows the experimental and calculated $\Psi(\lambda)$ and $\Delta(\lambda)$ curves for sample #5. One can see that $\Psi(\lambda)$ and $\Delta(\lambda)$ calculations within the single-layer model at zero extinction coefficient are in good agreement with experimental data. This is, somewhat, a surprising result, because the minimum extinction coefficient value determined by the SE measurements was less than 10^{-3}. The fact that extinction coefficient at $\lambda = 632.8$ nm for the HfO_x film #3 ($x = 1.67$) was 1.43, whereas for the film #4 ($x = 1.82$) it was less than 10^{-3}, indicates that optical properties of HfO_x films are strongly dependent on the x value.

According to XPS data [8], the non-stoichiometric HfO_x films consist of only three components: Hf metal clusters, Hf_4O_7 suboxide and stoichiometric HfO_2 (figure 4). The films of group 1 contain all three phases, and the films of group 2—only last two ones. The strong absorption in films containing metallic phase and their optical properties are similar to the pure metal surface optical properties. The transparent films of group 2 are the dispersion medium consisting of suboxide Hf_4O_7 and HfO_2 oxide, and, thus, films optical properties can be described in terms of the Bruggeman effective medium approximation

$$q \cdot \frac{\varepsilon_x - \varepsilon_{HfO_2}}{\varepsilon_{HfO_2} + 2\varepsilon_x} + (1 - q) \cdot \frac{\varepsilon_x - \varepsilon_{Hf_4O_7}}{\varepsilon_{Hf_4O_7} + 2\varepsilon_x} = 0, \quad (5)$$

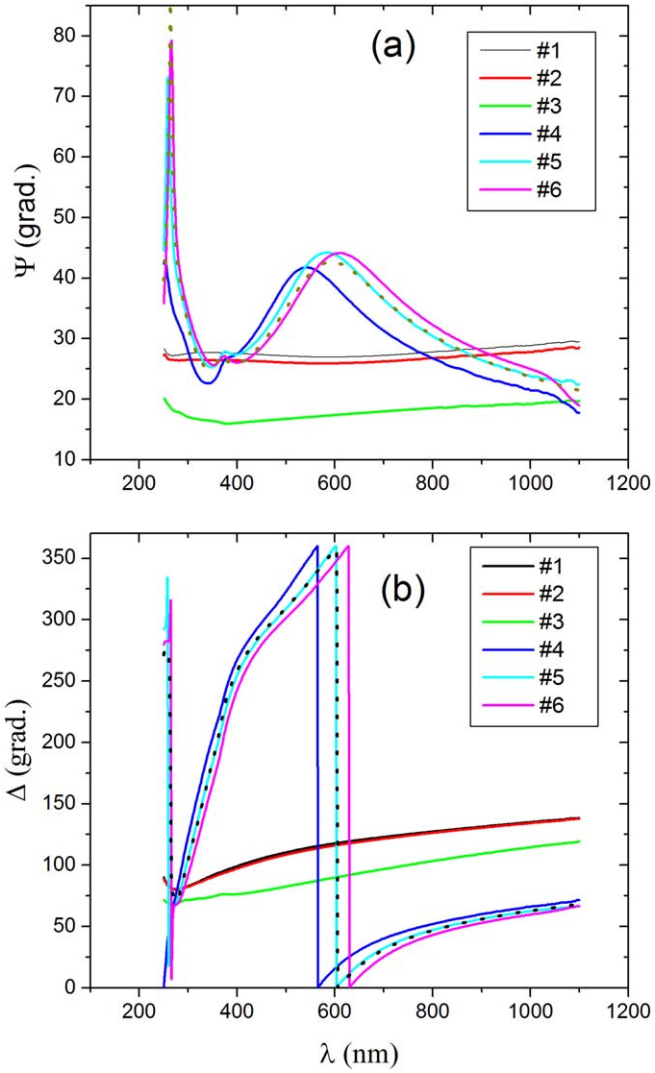

Figure 1. Experimental wavelength dependences of ellipsometric angles (a) Ψ and (b) Δ for samples #1–6. Dot lines—Ψ(λ) and Δ(λ) dependences for sample #5 calculated within the single-layer model framework.

where q and (1-q)—HfO_2 and Hf_4O_7 volume fractions in the insulating matrix according to XPS data (table 3), $\varepsilon_{HfO_2} = n^2_{HfO_2}$—$HfO_2$ dielectric constant ($k_{HfO_2} = 0$), $\varepsilon_{Hf_4O_7} = n^2_{Hf_4O_7}$—$Hf_4O_7$ dielectric constant ($k_{Hf_4O_7} = 0$), $\varepsilon_x = n_x^2$—effective medium dielectric constant ($k_x = 0$). Assuming the spectral dependence of the effective medium refractive index $n_x(\lambda)$ for samples #4 and #5 as $n(\lambda)$, the values of Cauchy polynomial coefficients for Hf_4O_7 and HfO_2 components were derived (table 3). Then the dependence $n_x(\lambda)$ for sample #6 was calculated using the effective medium approximation and taking into account the Cauchy polynomial coefficients for Hf_4O_7 and HfO_2. As can be seen in figure 3, the experimental dependence $n(\lambda)$ obtained from the ellipsometry data for sample #6 and $n_x(\lambda)$ calculated using the Bruggeman formula for this sample are nearly identical. The correlation between the refractive index and the x value of HfO_x films was calculated using the Cauchy coefficients for Hf_4O_7 suboxide and HfO_2 oxide at wavelength $\lambda = 632.8$ nm (figure 5). This linear dependence is of high practical importance as it allows estimating a chemical composition of HfO_x films using only the parameters obtained by the optical measurements of the films.

The experimental dependences $n(\lambda)$ and $k(\lambda)$ obtained by the method of spectral ellipsometry can be used to calculate reflection or transmission spectra. Figure 6 shows the reflection spectra of our structures, calculated using the OptiLayer program (OptiLayer GmbH). In order to show the effect on the reflection spectrum only the values of the chemical composition coefficient 'x', calculations were made for films of the same thickness.

Optical constants n(632.8 nm) and k(632.8 nm) HfO_x film with an oxygen concentration gradient along the 'Lx' direction, measured on a 'Microscan' ellipsometer, are shown in figure 7. It can be seen that a sharp jump in the optical constants is observed in the region $x \approx 1.8$. It is known that charge transfer in dielectric films of non-stoichiometric oxides of HfO_x is associated with oxygen vacancies [19]. Their concentration significantly affects the electrical conductivity of the films. At low vacancy concentrations of oxygen ($x \approx 1.82 \div 2.0$), the electrical

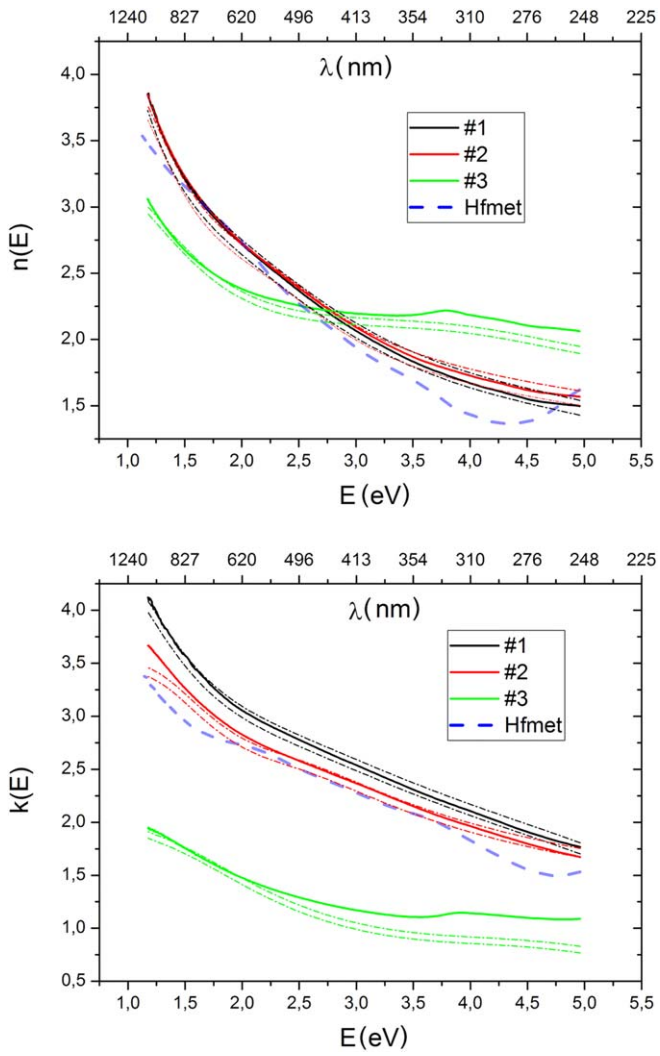

Figure 2. Optical constants $n(E)$ and $k(E)$ for opaque HfO_x films (group 1). Hf_{met}—optical constants for the metal hafnium surface.

Table 2. Thicknesses and parameters of the Drude-Lorentz model for opaque HfO_x films.

				Drude-Lorentz model parameters			
Sample	Film thickness (nm)	ε_∞	E_{1D} (eV)	E_{2D} (eV)	A_n	E_n (eV)	Γ_n
					18.15	0.87	1.09
#1	50.7	1.1	19.9	19.3	3.20	2.32	1.07
					0.23	4.89	1.16
#2	54.8	1.3	20.7	19.2	4.0	1.2	0.8
					1.0	2.3	0.6
#3	105.7	4.2	10.7	12.8	3.5	1.4	1.2
					0.6	4.0	0.6

conductivity of the films is described by the hopping mechanism [20]. With decreasing 'x' (an increase in the concentration of oxygen vacancies), the electrical conductivity increases. At higher concentrations of oxygen vacancies ($x < 1.82$), the dependence of electrical conductivity on 'x' can be described in terms of percolation theory [21]. Optical measurements investigate the high-frequency (ω–>∞) response of the Si(100)/HfO_x structure to the electromagnetic action (ω is the frequency of the electromagnetic wave), while the conductivity measurements of HfO_x films at a constant current is a low-frequency ($\omega \approx 0$) response. However, despite possible significant differences in the nature of these responses, we assume that the observed jump in the optical constants (n, k) at $x \approx 1.8$ is a consequence of the percolation transition in the electrical conductivity of the film. In accordance with the theory of percolation, the dimensions of conducting clusters increase with increasing concentration of oxygen vacancies. Probably, for $x > 1.82$ the dimensions of the conducting clusters in the film

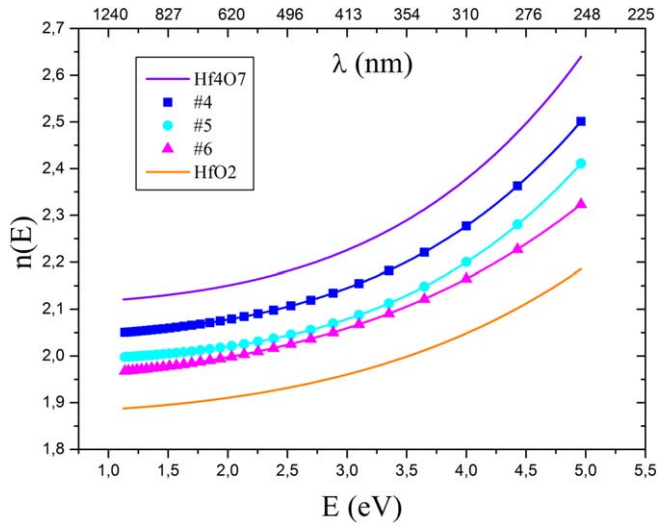

Figure 3. Refractive index spectral dependencies for samples #4–6 calculated within Bruggeman effective medium approximation (points). Two solid lines are refractive indexes for Hf_4O_7 and HfO_2 components.

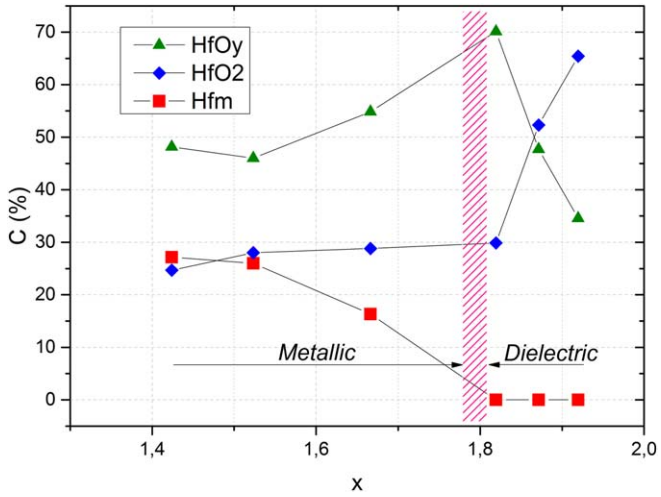

Figure 4. The HfO_x film chemical composition dependence on x value [8]. Hf_m, HfO_y and HfO_2 are concentration of the metallic phase, suboxide Hf_4O_7 and HfO_2 oxide, respectively. The films of group 1 are metallic, and the films of group 2 are dielectric ones. As distinct from [8], Hf_m is the total concentration of the metallic phase into the film volume and onto the film surface.

Table 3. Thicknesses and polynomial Cauchy coefficients for transparent HfO_x films.

Sample	Film thickness (nm)	Cauchy coefficients			Concentration of Hf atoms (XPS data) Hf_4O_7 + HfO_2
		a	$b\,(\times 10^{-2}\,\mu m^2)$	$c\,(\times 10^{-4}\,\mu m^4)$	
#4	75.7	2.040	1.165	10.725	70.1% + 29.9%
#5	84.5	1.989	0.895	10.881	47.7% + 52.3%
#6	89.5	1.955	1.481	5.147	34.6% + 65.4%
Components					
Hf_4O_7		2.110	1.208	13.125	
HfO_2		1.878	1.108	5.078	

are much smaller than the wavelength of the radiation, and the electromagnetic wave perceives the film as dielectric. Accordingly, the dependences of the optical constants n(λ) and k(λ) are dielectric in character and are described by the Cauchy formula. At $x < 1.82$, the dimensions of the conducting clusters exceed the wavelength of light, and the electromagnetic wave perceives the film as a metal, i.e. the optical constants $n(\lambda)$ and $k(\lambda)$ are metallic in nature.

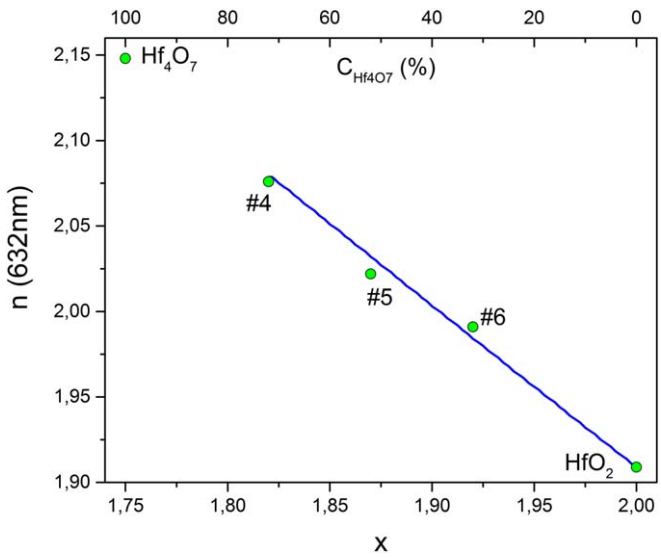

Figure 5. Dependence of refractive index n at $\lambda = 632.8$ nm on x value for transparent HfO_x films #4–6. C_{Hf4O7}—the concentration of Hf_4O_7 suboxide in the films.

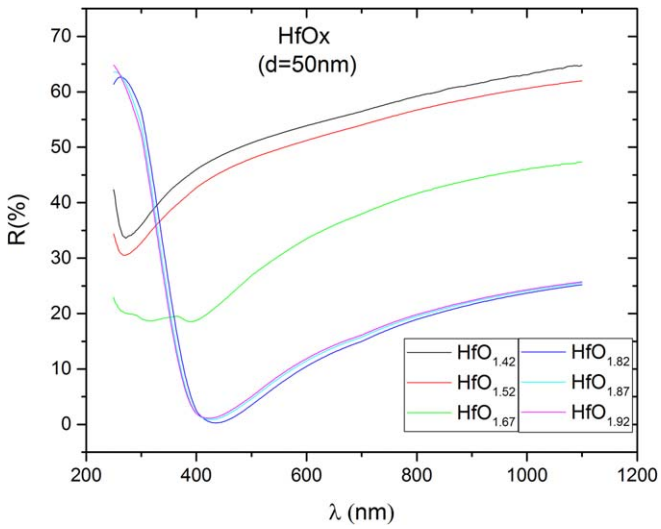

Figure 6. Calculated spectra of the reflection coefficient for Si (100) /HfO_x structures. d is the thickness of the film.

4. Conclusions

Non-stoichiometric HfO_x films of different chemical composition ($x < 2$) were fabricated by the IBSD method. The ratio of O and Hf atoms in the films, varied by setting the O_2 partial pressure in a chamber, was previously determined by XPS. In addition, a sample with a gradient x along the surface of the HfO_x film was prepared. In this work, the effect of chemical composition on the optical properties of the films was studied by spectroscopic ellipsometry methods in the $\lambda = 250$–1100 nm wavelength range. The spectral dependences of refractive index $n(\lambda)$ and extinction coefficient $k(\lambda)$ were found to undergo radical changes within $x = 1.78$–1.82. It was established that the transition from the metallic to the dielectric-like behavior of the optical constants occurs not smoothly, but is discontinuous, and a sharp jump in the optical constants is observed at $x \approx 1.8$. When $x < 1.78$, the films have a high extinction coefficient $k > 1$ and the behavior of optical constants spectral dependences is similar to those for metals. When $x > 1.82$ the films are transparent ($k = 0$). The metallic character of strongly absorbing films was compared with pure metal hafnium surface, and the optical properties of theses opaque films were described with the Drude-Lorentz model. The transparent (dielectric) film dispersions $n(\lambda)$ are well approximated by the Cauchy polynomial dependence. From films composition XPS data the Cauchy coefficients for suboxide Hf_4O_7 and oxide HfO_2 were derived by using Bruggeman effective

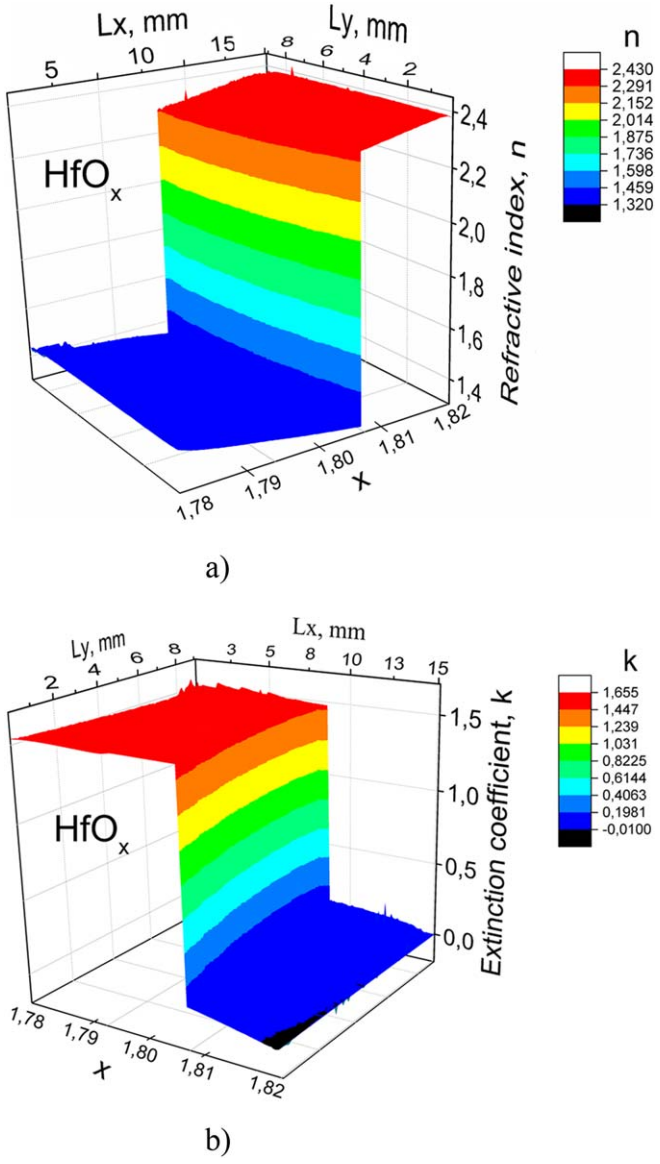

Figure 7. Refractive index $n(\lambda)$ (a) and extinction coefficient $k(\lambda)$ (b) maps at $\lambda = 632.8$ nm of a sample with a gradient of x over a scanning area of 15×10 mm^2. Lx is a concentration gradient direction of oxygen vacancies, x- the chemical composition coefficient of HfO_x film. Ly is a direction along width of the sample.

medium approximation. A good agreement of Hf_4O_7 and HfO_2 volumetric concentrations in the effective medium approximation with ones obtained from XPS data was established. The refractive index dependence on x value for transparent HfO_x films was calculated within the Bruggeman effective medium approximation for $1.82 < x < 2$. This dependence allows to estimate the chemical composition of HfO_x film from the optical measurements, which can be useful, for example, for the synthesis of functional layers of ReRAM structures.

Acknowledgments

This work was funded under project AAAA-A17-117042110141-5.

ORCID iDs

A K Gerasimova https://orcid.org/0000-0003-2932-8424
V Sh Aliev https://orcid.org/0000-0002-4266-971X
V A Voronkovskii https://orcid.org/0000-0001-5139-4394
S G Bortnikov https://orcid.org/0000-0002-7695-8499

References

[1] Takeuchi H, Ha D and King T J 2004 Observation of bulk HfO_2 defects by spectroscopic ellipsometry *J. Vac. Sci. Technol.* A **22** 1337
[2] Cho Y J, Nguyen N V, Richter C A, Ehrstein J R, Lee B H and Lee J C 2002 Spectroscopic ellipsometry characterization of high-*k* dielectric HfO_2 thin films and the high-temperature annealing effects on their optical properties *Appl. Phys. Lett.* **80** 1249
[3] Nguyen N V, Davydov A V, Chandler-Horowitz D and Frank M M 2005 Sub-bandgap defect states in polycrystalline hafnium oxide and their suppression by admixture of silicon *Appl. Phys. Lett.* **87** 192903
[4] Gallais L, Capoulade J, Natoli J Y, Commandre M, Cathelinaud M, Koc C and Lequime M 2008 Laser damage resistance of hafnia thin films deposited by electron beam deposition, reactive low voltage ion plating, and dual ion beam sputtering *Appl. Opt.* **47** 107
[5] Yang J J, Pickett M D, Li X, Ohlberg D A, Stewart D R and Williams R S 2008 Memristive switching mechanism for metal/oxide/metal nanodevices *Nat. Nanotechnol.* **3** 429
[6] Bersuker G *et al* 2011 Metal oxide resistive memory switching mechanism based on conductive filament properties *J. Appl. Phys.* **110** 124518
[7] Fang Z, Yu H Y, Liu W J, Singh N and Lo G Q 2010 Resistive RAM based on HfO_x and its temperature instability study *World Acad. Sci. Eng. Technol.* **48** 905
[8] Aliev V S, Gerasimova A K, Kruchinin V N, Gritsenko V A, Prosvirin I P and Badmaeva I A 2016 The atomic structure and chemical composition of HfO_x ($x < 2$) films prepared by ion-beam sputtering deposition *Mater. Res. Express* **3** 085008
[9] Fujiwara H 2007 *Spectroscopic Ellipsometry: Principles and Applications* (West Sussex, U. K: Wiley)
[10] Jellison G E Jr 1998 Spectroscopic ellipsometry data analysis: measured versus calculated quantities *Thin Solid Films* **313** 33
[11] Bao X, Muhler M, Schedel-Niedrig T and Schlögl R 1996 Interaction of oxygen with silver at high temperature and atmospheric pressure: a spectroscopic and structural analysis of a strongly bound surface species *Phys. Rev.* B **54** 2249
[12] Ramana C V, Utsunomiya S, Ewing R C, Becker U, Atuchin V V, Sh A V and Kruchinin V N 2008 Spectroscopic ellipsometry characterization of the optical properties and thermal stability of ZrO_2 films made by ion-beam assisted deposition *Appl. Phys. Lett.* **92** 011917
[13] Atuchin V V, Kruchinin V N, Kalinkin A V, Sh A V, Rykhlitskii S V, Shvets V A and Spesivtsev E V 2009 Optical properties of the $HfO_{2-x}N_x$ and $TiO_{2-x}N_x$ films prepared by ion beam sputtering *Opt. Spectrosc.* **106** 72
[14] Ramana C V, Mudavakkat V H, Bharathi K K, Atuchin V V, Pokrovsky L D and Kruchinin V N 2011 Enhanced optical constants of nanocrystalline yttrium oxide thin films *Appl. Phys. Lett.* **98** 031905
[15] Werner W S, Glantschnig K and Ambrosch-Draxl C 2009 Optical constants and inelastic electron-scattering data for 17 elemental metals *J. Phys. Chem. Ref. Data* **38** 1013
[16] Rykhlitskii S V, Spesivtsev E V, Shvets V A and Prokop'ev V Y 2009 Scanning ellipsometric setup 'MICROSCAN-3M' *INET* **3** 155 [in Russian]
[17] Amirtharaj P M 1985 *Handbook of Optical Constants of Solids* (San Diego, CA: Academic)
[18] Tompkins H G and Irene E A 2005 *Handbook of Ellipsometry* (Norwich, NY: William Andrew)
[19] Perevalov T V, Aliev V S, Gritsenko V A, Saraev A A and Kaichev V V 2013 Electronic structure of oxygen vacancies in hafnium oxide *Microelectron. Eng.* **109** 21
[20] Islamov D R, Gritsenko V A, Cheng C H and Chin A 2014 Origin of traps and charge transport mechanism in hafnia *Appl. Phys. Lett.* **105** 222901
[21] Kruchinin V N, Aliev V S, Perevalov T V, Islamov D R, Gritsenko V A, Prosvirin I P and Chin A 2015 Nanoscale potential fluctuation in non-stoichiometric HfOx and low resistive transport in RRAM *Microelectron. Eng.* **147** 165